5-2018

Impact Ignition Mechanisms and Sensitization of an Aluminized Fluorinated Acrylic (AlFA) Nanocomposite

Ian A.J. Shelburne
Purdue University

IMPACT IGNITION MECHANISMS AND SENSITIZATION OF AN ALUMINIZED FLUORINATED ACRYLIC (ALFA) NANOCOMPOSITE

by

Ian A.J. Shelburne

A Thesis

Submitted to the Faculty of Purdue University

In Partial Fulfillment of the Requirements for the degree of

Master of Science in Aeronautics and Astronautics

School of Aeronautics & Astronautics

West Lafayette, Indiana

May 2018

THE PURDUE UNIVERSITY GRADUATE SCHOOL
STATEMENT OF COMMITTEE APPROVAL

Dr. Steven F. Son, Co-Chair
Department of Mechanical Engineering
Dr. Ibrahim E. Gunduz, Co-Chair
Department of Mechanical Engineering
Dr. Davin Piercey
Department of Materials Engineering

Approved by:
Dr. Weinong Chen
Head of the Graduate Program

ACKNOWLEDGEMENTS

I would like to thank M.T. Beason for his support with the light gas gun and the Asay Shear Impact tests and for showing me the ins and outs of the lab during my first few months. I would also like to thank my advisors, Dr. Steven Son and Dr. Ibrahim Gunduz for their support and guidance through this project. This work was supported by the U.S. Army Armament Research Development Engineering Center.

TABLE OF CONTENTS

LIST OF TABLES

LIST OF FIGURES

ABSTRACT

Author: Shelburne, Ian, A.J. MSAAE
Institution: Purdue University
Degree Received: May 2018
Title: Impact Ignition Mechanisms and Sensitization of an Aluminized Fluorinated Acrylic (AlFA) Nanocomposite
Major Professor: Steven Son

Tailoring the reliability of impact ignited reactive materials continues to be an elusive challenge. Ideally, a sensitizing agent is preferred over device or reactive ingredient modification. Here, we report Asay shear impact studies of aluminized fluorinated acrylic (AlFA) and material sensitization via the introduction of inert particles. Initial Asay shear impact testing of neat $AlFA_{50}$ yielded a general baseline for material ignition at approximately 120 m/s for the configuration considered. Ignition was observed to occur on the far wall or in corners indicating that a pinching mechanism may be responsible. A modified experimental setup was used to image the response of a designed pinch point. Based on insights from these experiments, $AlFA_{50}$ samples were prepared with 15% glass beads by volume and were impacted at high and low velocities. Ignition events were then observed at velocities at least as low as 35 m/s and originated in the region of the face of the plunger rather than in corners. Further experiments with varying concentrations of the glass bead additives (between 10-30%) showed that the concentration could alter the level of sensitization of the material to low-speed impacts. The addition of glass micro-balloons was also considered but found to be less effective than glass beads. These results show that the impact sensitivity of these $AlFA_{50}$ materials can be tailored by the addition of inert beads, such as the glass beads used here, to create multiple pinch points in the reactive that can result in ignition. The work presented in this thesis serves to increase the understanding of the ignition of aluminum-fluorocarbon reactive materials to mechanical stimuli.

CHAPTER 1. INTRODUCTION

Energetic materials are a class of compounds which may undergo rapid exothermic reactions producing large amounts of heat and gases without the need for external oxidizers. These compounds, such as gunpowder, HMX, RDX, PETN…etc., have many commercial and military applications as pyrotechnics, explosives, and propellants. With the large amounts of energy these materials can store, there are often inherent dangers with their handling and use. External stimuli in the form of high and low speed impacts may inadvertently cause ignition or detonation of these materials resulting in damage or loss of life [1]. Some uses for energetic materials rely on impacts to ignite or detonate, and in these situations, reliability of impact ignition is critical. Ignition from an impact event is assumed to result from hot spot formation (localized energy dissipations) that are cause by several internal phenomena such as adiabatic shear, void collapse, particle fracture, viscous flow, or friction [2, 3]. These phenomena have been studied extensively and depending on the material and the impact mechanisms, one or more can be dominant in the formation of the hotspot [4]. In the particular impact setup and material configuration being investigated, adiabatic shear, void collapse, and viscous heating are likely to be the dominant hot spot formation mechanisms.

Understanding the impact ignition mechanisms which newly synthesized energetic materials are most susceptible to is critical to determining where they may be utilized. For materials that are considered for impact ignition applications, understanding the mechanics behind the ignition opens up the possibility of tailoring the sensitivity of the material for a broader range of scenarios. Experimental results from this work will aid in the understanding of the low speed impact ignition mechanisms for a newly synthesized reactive polymer material.

The work presented aims to investigate the mechanisms leading to low-speed impact ignition and sensitization of an aluminized fluorinated acrylic (AlFA) nanocomposite. Results will then be used to tailor the impact induced ignition through the addition of inert particles to the material.

1.1 Hot Spot Formation and Impact Ignition Mechanisms

It has been shown that the energy from many low to high speed impacts is not great enough to cause ignition without intermediate phenomena that localize energy [3]. Previous work in the field of impacted energetic materials has shown that energy localization through hot spot formation is the primary contributor to successful impact ignition [2,3,5-9]. There are several mechanisms responsible for the formation of hot spots, such as adiabatic shear, cavity collapse, and viscous heating. Each of these mechanisms is independent from one another but can occur simultaneously depending on the material and impact configuration.

The deformation of some energetic materials from an impact has been observed to occur in localized regions of high strain, referred to as shear bands [2,3,7,10,11]. This adiabatic shearing of the material is a result of a buildup and of a large number of dislocations along the slip planes of the impacted solid. Once there are a significant amount of dislocations built up on one slip plane, it becomes energetically favorable for the dislocations to move to another slip plane, releasing localized energy. The buildup and release of dislocations can occur in rapid succession, releasing large amounts of localized energy forming shear bands and causing material ignition [4,7,12]. High speed imaging of impacted PETN has shown ignition events originating within the shear band of the deforming sample as seen in Figure 1.1 [2].

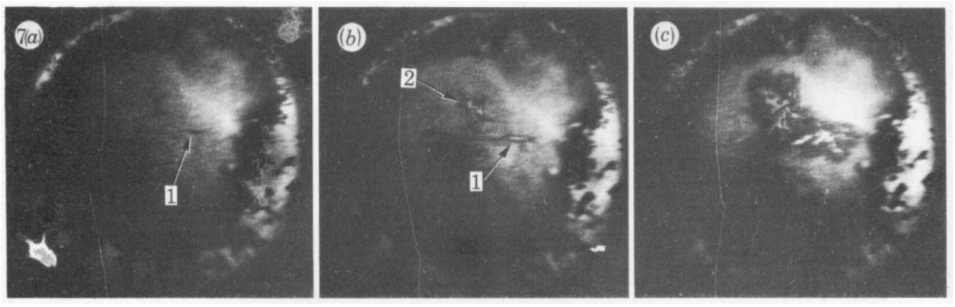

Figure 1.1: From left to right progress through an impact scenario of PETN. Shear bands, highlighted by [1] and [2] can be seen as the points of initiation that continue to c) [2].

Energetic materials can also be ignited through viscous heating which occurs in regions of high shear. Dissimilar to adiabatic shear, these regions occur at pinch points where material is being rapidly extruded between two or more surfaces. In these regions, viscoplastic work is being

done on the material which results in a rise in temperature. In these regions of high shear, friction might also add to the heating of the material.

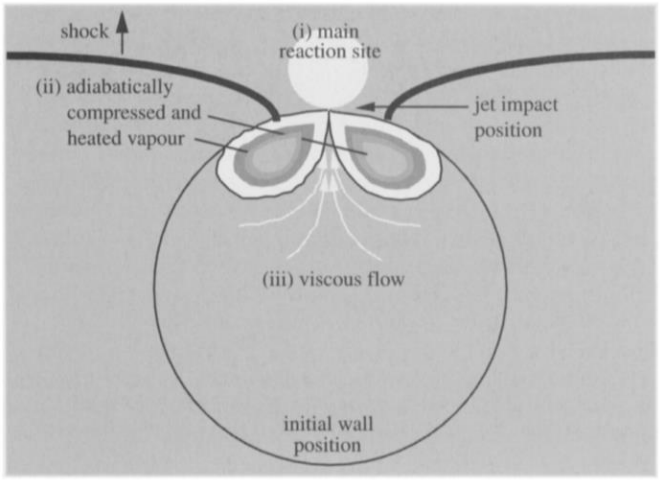

Figure 1.2: Schematic of a shock collapsing a cavity. Jetting of material from the initial wall position to the final is the main cause for hot spot formation at the main reaction site [13].

Hot spot formation may also occur due to cavity collapse within materials where voids are present as a result of three distinct phenomena: viscoplastic heating, material jetting, and adiabatic heating of void gases. Viscoplastic heating occurs along the outside region of the void structure from the viscoplastic work on the material as the void is collapsed [14]. Heating of the void wall can occur due to high speed impact (shock event) when material is compressed and jetted across the void at high speed, impacting the opposite wall [13,14]. Adiabatic heating occurs due to the rapid collapse of the void around the trapped gases within. Each of these three effects play a role in the overall formation of hot spots from void collapse and can be seen in Figure 1.2. Because jetting is more likely to occur in shocked materials, void collapse may not be a dominant hot spot mechanism in non-shocked impacts [4,13]. Additionally, shocked energetic materials have the potential to be sensitized through the addition of voids, such as the addition of micro-balloons in liquid explosives [15,16]. This addition allows some materials to be tailored to different scenarios, increasing their possible uses.

1.2 Fluoropolymer Energetic Materials

Fluoropolymers have been actively explored as oxidizers and reactive binders in a variety of energetic formulae starting shortly after their invention in the 1930's. Fluorine, a strong electronegative element, reacts well with strong electropositive metals such as aluminum. The reaction between fluorine and aluminum, similarl to aluminum and oxygen, produces large amounts of energy. Besides being good oxidizers, fluoropolymers when combined with energetic systems allow for enhanced mechanical properties, thermal stabilities, and chemical resistance [17]. One common fluoropolymer used in energetic materials is Polytetrafluoroethylene (PTFE), also known as Teflon, which was first invented by DuPont in the late 1930's. Since then, preparations of PTFE with electropositive elements such as magnesium, silicon, and aluminum have produced energetic materials with highly exothermic reactions producing flame temperatures in excess of 3000 °C.

The dual role of fluoropolymers as binders and coatings adds to their desire in energetic materials. Fluoropolymers have been used as substitutes for hydrocarbon binders in solid rocket fuels and as a result, it was seen that there was an increase in the thermal stability of the fuel [18]. As a coating, fluoropolymers have been used to passivate aluminum particles, reducing their pyrophoric nature as well as reducing the impact sensitivity of certain thermites [19,20].

Recent work has been done towards the development of a novel nano-aluminum fluoropolymer at the Air Force Research Laboratory (AFRL). Prepared through *in-situ* polymerization of perfluorodecyl methacrylate (PFDMA) with PAM functionalized nano Al, aluminized fluorinated acrylic or AlFA has been shown to exhibit self-sustaining combustion at 50/50 Al/Polymer configuration [21]. This configuration, also known as $AlFA_{50}$ which is machinable and moldable has shown good thermal stability and low sensitivity to impact and friction. A "pinch point" has been used to describe the primary cause for material ignition in impact events [22]. The low sensitivity and machinability makes $AlFA_{50}$ a good candidate for a variety of uses as an energetic material.

CHAPTER 2. EXPERIMENTAL METHODS

2.1 Test Section Preparation

Delrin®, or polyoxymethylene, stock rod was machined into cylindrical projectiles 25.35 (diameter) x 31.75 mm (length) and 1018 steel was machined into a disk 20.37 (diameter) x 3.18 mm (height). The steel disk was press fit into the top lip of the Delrin sabot to act as the impact delivery mechanism into the Asay shear test fixture (See Figure 2.1). A steel sample retention plate was machined to 50.8 (height) x 57.15 (length) x 2 mm (thick) with a 20.32 (height) x 42.67 mm (length) slot formed along the lengthwise axis. Steel was machined into backplates, 12.5 mm (thick), and front plates, 9.5 mm (thick) with a 25.4 mm (diameter) hole located along the lengthwise axis with a center point 25.4 mm from one of sides, with the same height and length as the retention plate. A window retention plate was machined 2.5 mm (thick) with a 21.43 mm (diameter) hole located similarly to the holed front plate. Acrylic 25.4 mm (diameter) was machined and polished clear into 9.5 mm (thick) windows and press fit into the front plates. Rectangular plungers were machined 20 (height) x 31.75 (length) x 2 mm (thick) to transfer the impact from the projectile into the samples. The four pieces were assembled and held together with four 1.25 in. ½ - 20 screws with four ½ - 20 jam nuts through four 7.14 mm (diameter) through holes located in each corner as shown in Figure 2.1.

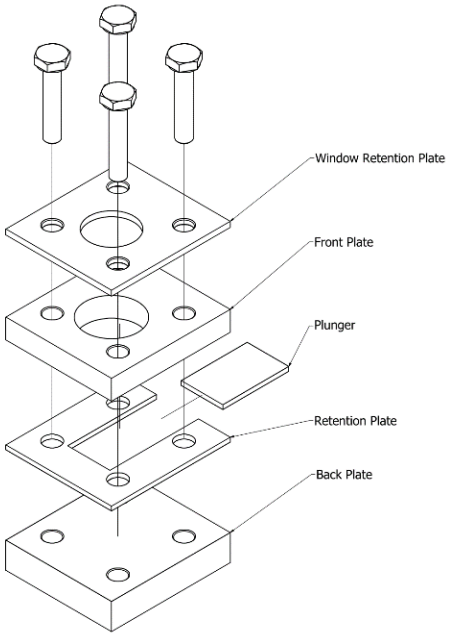

Figure 2.1: Exploded assembly view of the test section used during the Asay shear tests.

2.2 Sample Preparation

Neat $AlFA_{50}$ samples were received in the form of pressed pellets and hand molded cones from US Army Armament Research Development and Engineering Center (ARDEC). The pressed $AlFA_{50}$ pellets were dimensioned with a digital micrometer and weighed and a nominal density of 2.14 g/cm^3 was calculated. Received samples were hand ground down in a large mortar and pestle to a coarse powder and were stored in a plastic container prior to use. M15 micro-balloon fillet material from Goldenwest Mfg. was found to have a nominal density of 0.075 g/cm^3. Small glass beads were sieved for a size greater than 1mm and were found to have a nominal density of 2.5 g/cm^3.

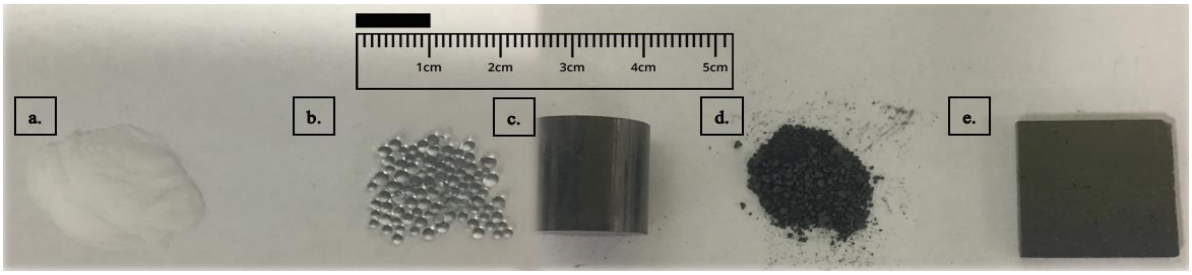

Figure 2.2: a) glass micro-balloons b) glass beads c) $AlFA_{50}$ pellet d) ground $AlFA_{50}$ e) molded $AlFA_{50}$

A mold was created with a back plate, retention plate, and plunger (Figure 2.3a) and placed onto a digital hot plate set to maintain a temperature of 180 °C. Enough neat crushed $AlFA_{50}$ to form a 20 x 20 x 2 mm sample was massed on a digital scale and then placed into the heated mold. As the $AlFA_{50}$ sample was heated, it was worked to remove any voids and pressed into the mold with a flat metal spatula. The mold was removed from the heat and allowed to cool before the sample was removed and individually bagged for storage. Filler material was hand mixed with the granulated $AlFA_{50}$ material in varying quantities before molding to create samples with $AlFA_{50}$ at 70-90% by volume with the glass beads and 65-90% by volume with micro-balloons. These samples were molded with the same methods and to the same dimension as the neat $AlFA_{50}$ samples. Neat crushed $AlFA_{50}$ was massed to create samples 20 x 10 x 2 mm in size and were molded as before except with the plunger closer to the back wall of the retention plate (Figure 2.3B).

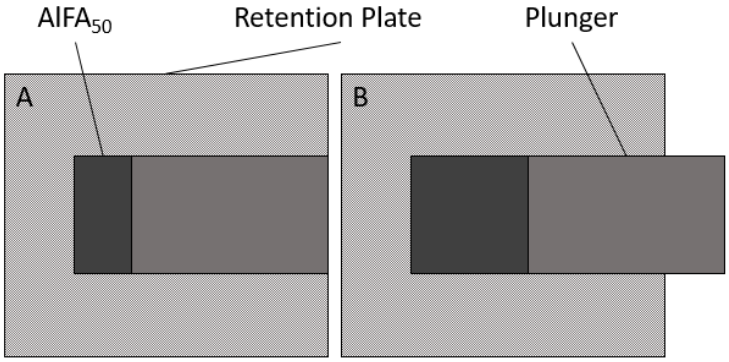

Figure 2.3: Half A) and full B) sized sample mold configuration for $AlFA_{50}$ casting.

2.3 Asay Shear Impact Experiments

Samples were loaded into the sample holders so that they were flush against the back wall of the retention plate. Each test section was closed with the front plate and window retention plate and held loosely together with the ½ - 20 screws and jam nuts. Plungers were placed into the opening of the retention plate and pushed flush against the edge of the sample. The nuts were tightened just enough that the sample held together but did not impede the sliding of the plunger. The Delrin projectiles were loaded into the breach section of a single stage light gas gun [23-25]. The sample holders were placed into the steel anvil mount with shims being used to align the

holder with the barrel of the gas gun. A large steel anvil backstop that was bolted in place was used to prevent the sample holder from being ejected from the mounting anvil after being struck by the projectile. A quick release valve was pressurized with nitrogen and was used to rapidly open a plenum chamber containing pressurized helium propelling the sabot towards the sample. A xenon arc lamp was used to illuminate the sample holder through the acrylic window. A phantom v7.3 high speed camera with a Nikon macro lens was used to capture high speed images of the impact event as seen through the window retention plate and acrylic window, a 21.43 mm viewing diameter. Manual triggering of the high speed camera was used to capture the video after the gas gun was successfully fired. The velocity of the plunger moving through the $AlFA_{50}$ samples was measured using the viewing window as a reference distance and then tracking the location of the plunger face for several frames. A schematic of the gas gun and key components can be seen in Figure 2.4.

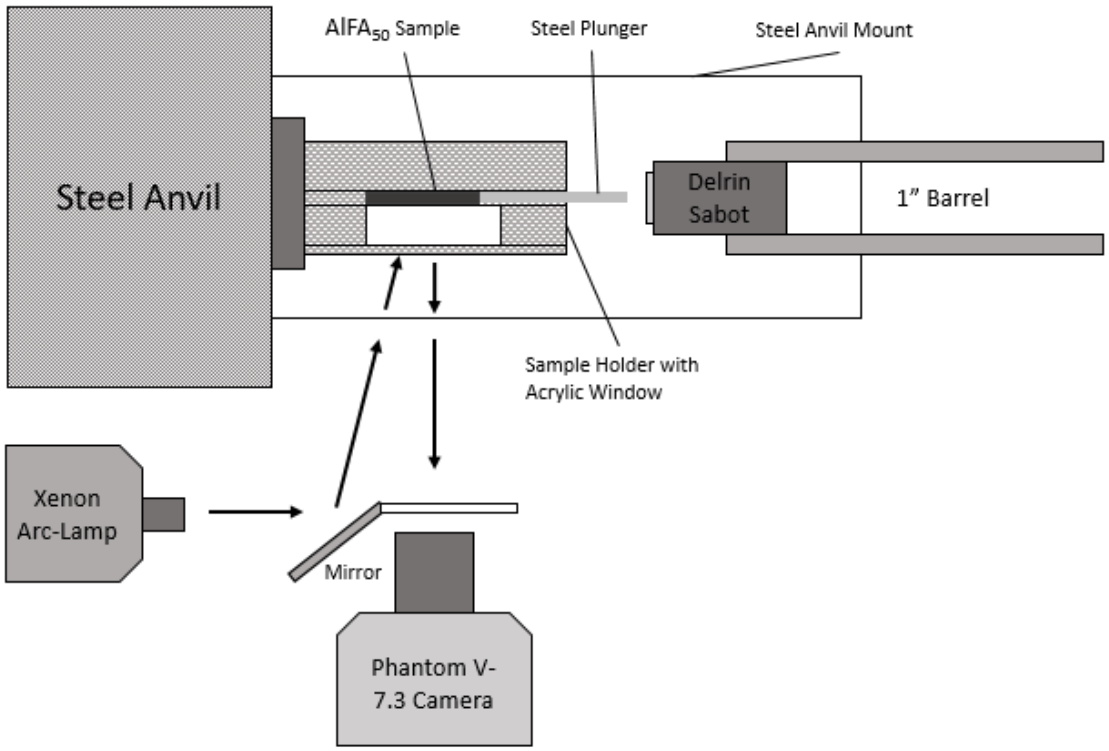

Figure 2.4: Schematic of the light gas gun's key components as seen from a top view. The position of the mirror varied from test to test to best illuminate the sample.

A Matlab video analysis script was written and employed as a method to determine the time to ignition. Each frame of video was broken down into four columns of equal size with the right and left most columns of pixels being excluded from analysis as they were outside the area of interest. The average pixel intensity of the center two columns was measured on a scale from 0-252 during each frame and was offset by the initial pixel intensity of the image before impact. Ignition delay was measured from the impact time to the time the average pixel intensity of the middle two columns surpassed an arbitrary threshold.

CHAPTER 3. RESULTS AND DISCUSSIONS

3.1 Material Behavior

Figure 3.1 shows a sequence of profile images of the test section during a successful ignition of neat $AlFA_{50}$. In these images, the events preceding and including the ignition of a sample of neat $AlFa_{50}$ at a high impact velocity (121 m/s) is shown. A successful impact event can be broken into three distinct phases: impact and radial expansion, penetration and extrusion, then ignition. A close examination of the individual frames in Figure 3.1 provides a better description of what each of these phases of the impact event entail. Between the first two frames, the plunger begins to compress the $AlFA_{50}$ causing it to expand radially to fill any excess gap between it and the walls. From frame three until the point of ignition, the plunger continues to travel through the sample towards the back wall of the test section. Finally, in the last frame at 220 μs, ignition (indicated by light emission) of the sample is seen originating from the back of the test section where the plunger has met the back wall. In a previous study, it was shown that $AlFA_{50}$ ignites when "there is little or no visible gap between the projectile and the back wall," that is a "pinch point" is developed [22]. At these pinch points, there are regions of high shear within the material which may induce the temperature rise required for ignition due to viscous heating effects. The locations of these pinch points in successful impact experiments of neat $AlFA_{50}$ were not readily visible.

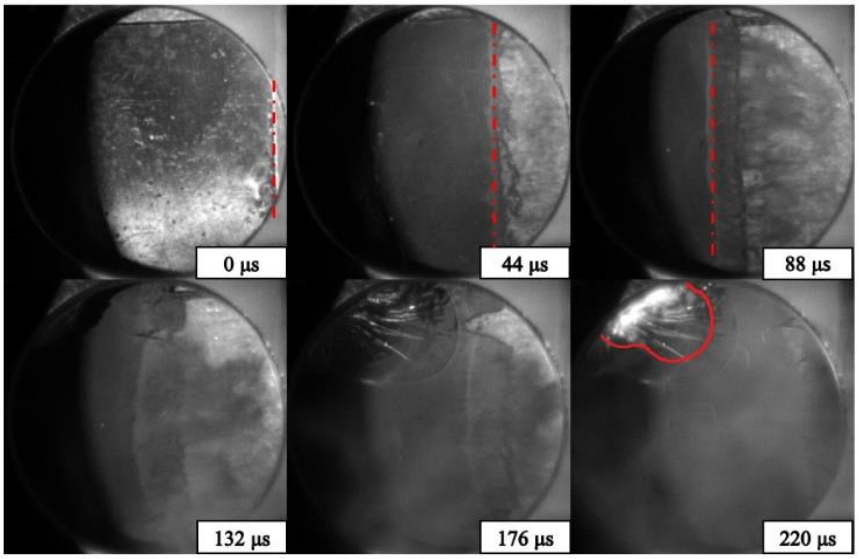

Figure 3.1: Asay impact experiment on neat $AlFA_{50}$ at a plunger velocity of 121 m/s. The location of the face of the plunger is indicated by the dashed lines. Ignition of the $AlFA_{50}$ material can be seen in the top right corner of the final frame at approximately 220 µs after initial plunger impact. Dotted lines are used to indicate the approximate plunger face location during each frame and solid lines are used to highlight ignition sites.

During the primary and secondary phases of this impact event, the sample is seen to remain largely in one piece, unless ignition occurs, even though it is brittle and being strained at a high rate. In all images post impact where reaction has not occurred, the material appears to deform as if it is a high viscosity liquid, which may be due to heat generated from the initial impact, causing the $AlFA_{50}$ to partially melt. Previous studies by White et al. [18-paper] noted similar observations which were attributed to the high polymer matrix content. The "melting" of the sample rapidly reduces the velocity of the plunger as it is forced to travel through a viscous medium also forcing the extrusion of the material between the plunger and the test section wall. Reduction of the plunger velocity could prevent pinch points from forming along the back wall, reducing the chance of a successful ignition. Low impact velocities (81 m/s) in the same configuration as those in Figure 3.1 were unsuccessful in causing ignition of the sample. Inspection of recovered test sections showed that the plunger had, in all cases, failed to penetrate all the way through the material to the theorized pinch point location.

Investigation of the pinch point as a mechanism for ignition was conducted with the alternative backplate setup as seen in the right side of Figure 3.2. The left side of Figure 3.2 shows two impact events at 91 m/s and 127 m/s where several of the phenomenon described earlier can be clearly seen. In the middle frame of each test, the impact is seen to melt material which then can be seen flowing around the backplate and into the corners. The final frame of each test clearly shows that the ignition point is located where the plunger and the rounded backplate have come into complete contact to form a well-defined pinch point. These tests indicate that a pinching mechanism for these materials can lead to effective hot spot formation and ignition. Addition of this type of pinch point could be accomplished through a mechanical device or specific configuration, however in many applications it would be preferred and possibly simpler, to modify the material with an inter fill.

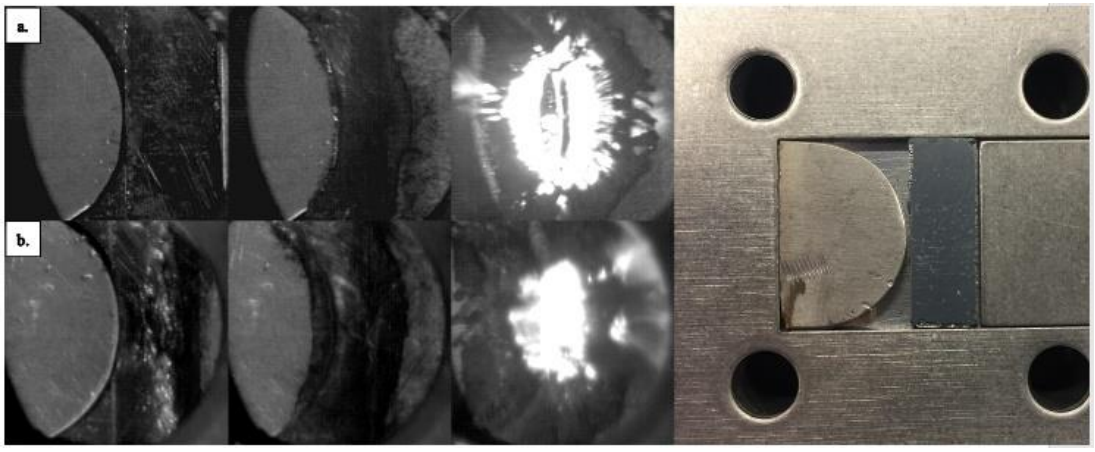

Figure 3.2: Impact event of neat $AlFA_{50}$ with a modified backplate and the configuration of the test. Left: ignition of $AlFA_{50}$ at the pinch point at an impact velocity of a) 127 m/s and b) 91 m/s. Right: Semicircular backplate and half sized $AlFA_{50}$ configuration.

3.2 Sensitization

As a classical means of sensitizing liquid explosives, glass micro-balloons were selected as a candidate to sensitize $AlFA_{50}$ to impact in this configuration. Glass beads were also considered. Prepared samples were categorized by the percentage of $AlFA_{50}$ by volume and were tested at high and low impact velocities to determine if ignition occurred and the time to ignition.

Time to ignition, or time to first light, was measured from the time of impact to the time visible light was seen emitting from the impacted material.

Of the twelve experiments performed at various additive percentages, only one test produced a result where the samples had been successfully sensitized to impact with the micro-balloons. In Figure 3.3 the array of images shows a high velocity impact of a 90% $AlFA_{50}$ by volume sample with micro-balloons reacting after successful sensitization. 45µs after initial impact, several ignition sites can be seen which continue to propagate into the next frame resulting in a successful ignition. In this sample, the ignition point has successfully been moved from the pinch point at the back of the test section to the front face of the plunger, and the time to ignition was greatly reduced. While some sensitization with the micro-balloons was achieved, the reliability and repeatability in the samples' configuration and plunger speed was poor.

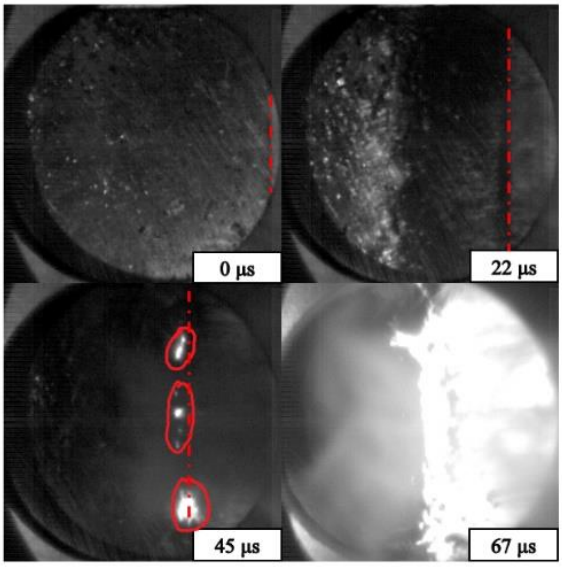

Figure 3.3: Prompt ignition of $AlFA_{50}$ samples with 10% micro-balloons by volume at initial plunger velocity of 142 m/s. The location of the face of the plunger is indicated by dashed lines. Ignition event can be seen occurring right along the face of the plunger approximately 45 µs after initial impact. Dotted lines are used to indicate the approximate plunger face location during each frame and solid lines are used to highlight ignition sites.

Examination of the results of unsuccessful samples as summarized in Table 3.1, shows the overall unreliability in the decrease of ignition time. Also, when studying the high-speed footage

from each of the successful ignition events, the most typical cause for ignition remained the pinch point at the back of the test section. Furthermore, samples impacted at even lower velocities showed no response to the addition of the micro-balloons as there were no successful ignition events. Recovery of the test sections of the unsuccessful trials presented further evidence for the melting and slowing of the plunger as seen in Figure 3.4. Sample MB-10 gives some idea as to the scale that is required for a successful pinch point as the remaining material between the plunger face and the back of the test section is less than 2 mm.

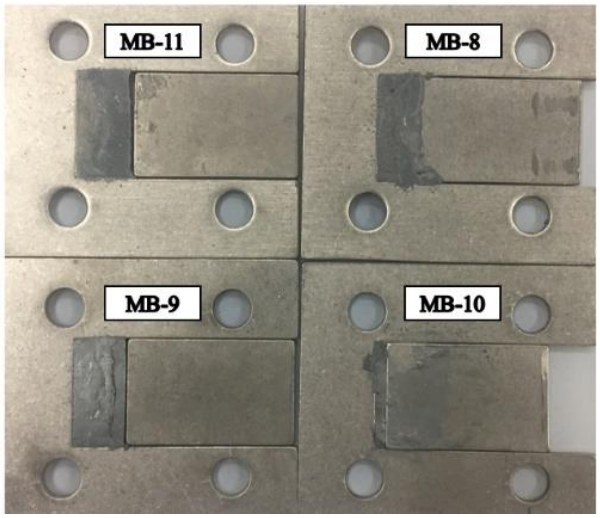

Figure 3.4: Recovered test sections from low velocity impacts of $AlFA_{50}$/Micro-balloon samples.

In summary, the addition of glass micro-balloons in both high and low speed tests did not show significant and consistent beneficial results. Although glass micro-balloons are a classic additive in liquid explosive sensitization, they mainly work through a void collapse process by which a strong shock collapses the void forming a hot spot. At 120 m/s impact velocities, the compression created by the impact of the plunger through the material is apparently not enough to successfully collapse enough voids fast enough to ignite the samples.

Table 3.1: Asay shear impact test results for $AlFA_{50}$/Micro-balloon samples at high and low velocities. The error on time to ignition is estimated to be 15-20 μs based on the frame rate of the camera.

Sample	% $AlAF_{50}$	Plunger Velocity (m/s)	Ignition	Time to Ignition (μs)
MB-1	89.47	135	Yes	174
MB-2	90.37	131	Yes	231
MB-3	90.98	142	Yes	43
MB-4	84.88	N/A	Yes	N/A
MB-5	85.36	111	Yes	266
MB-6	84.65	126	Yes	200
MB-7	83.92	122	Yes	261
MB-8	87.29	82	No	N/A
MB-9	82.80	53	No	N/A
MB-10	82.32	101	No	N/A
MB-11	64.49	65	No	N/A
MB-12	64.40	116	Yes	95

Sensitization of the $AlFA_{50}$ via the inclusion of glass beads was also examined, motivated by the evidence of pinch point induced ignition. Samples were characterized by percentage of glass beads included by volume and were studied at 70, 80, 85, and 90% $AlFA_{50}$ by volume. Tests were performed at high and low velocity impacts to characterize sensitization effects, ignition location, and ignition delays. Previously, time to ignition was measured by time to first light breaking out to the surface. Due to the optical properties of the glass beads, in some tests it was possible to see through the material, like a lens, and witness ignition events taking place on the back side of the samples. The inconsistency of the ability to see through the sample from test to test made it necessary to use an integrated video analysis, in the form of the pixel intensity identifying Matlab script, instead.

The array of images in Figure 3.5 shows the typical results from a variety of impact velocities of 85% $AlFA_{50}$ samples with glass bead additives. At all impact velocities, ignition of the samples was seen to occur in the region along the face of the plunger roughly midway through

the sample. This was observed consistently in all other test performed as well. As a result of the shift in ignition location, the time to ignition was observed to decrease dramatically in the glass bead loaded samples when compared to similar velocities of neat $AlFA_{50}$. In each observed test, the secondary phase of the impact event (penetration and extrusion), as described previously, was either minimal or nonexistent. Ignition events begin promptly after the sample material has filled the excess space of the test section during the primary phase and the impact velocity required to instigate an ignition event decreased. A minimum velocity of 35 m/s was observed (lowest speed that could be obtained for this setup), far lower than the minimum velocity of the neat material samples.

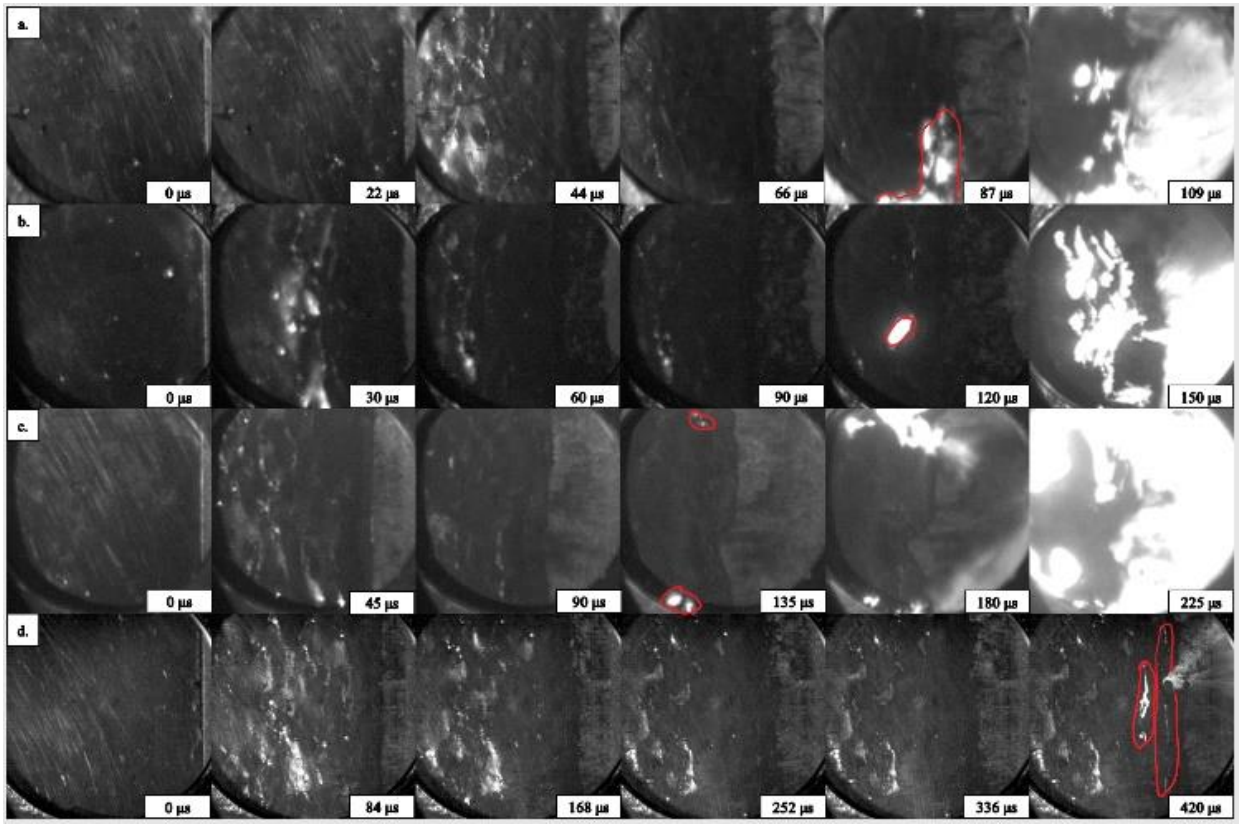

Figure 3.5: Impact ignition of 85% $AlFA_{50}$ by volume with glass beads at a) 124 m/s, b) 105 m/s, c) 69 m/s, and d) 35 m/s impact velocity. Ignition sites can be seen in the region along the face of the plunger as highlighted by the solid lines.

The primary mechanism for material ignition as described previously plays the same role in each of these tests. There are two possible mechanisms which lead to the pinch points which are

a direct result of the inclusion of the glass beads in the sample. The first possible pinch point comes from the interaction of individual glass beads during the primary phase. As the beads are pushed towards the back of the test section they are pressed together, and local regions of high shear occur resulting in hot spots and ignition. With this, it is expected that the larger addition of beads would result in increased sensitivity as more pinch points would occur. The second possible pinch point comes from the interaction of the plunger face and the compacted glass beads. During this primary phase, the glass beads are pressed together and begin to stack up producing an effective wall. Once the wall is sufficiently dense, the impinging plunger face creates a pinch point with the beads resulting in a region of high shear and therefore ignition. Similar to the first described pinch point event for this glass filled material, this too would benefit from an increase in the additive materials as it would take less time for a sufficient wall of glass beads to pileup. Results from samples at 70, 80, and 90% $AlFa_{50}$ were found to be qualitatively similar to those of the 85% samples. In each case, reaction initiation was in the region near the face of the plunger and lower plunger velocities were observed to cause successful ignition. The plots in Figure 3.6 show the overall trends observed between the ignition delay from initial impact and the impact velocity. A clear trend can be observed between each of the samples as the ignition delay decreases with an increase in the volume of additive glass beads showing clear tunability potential. These plots support the previous thought that an increase in glass beads (lower AlFA content) would result in an increase in bead to bead pinch point, as well as a decrease in the time required for the beads to densify to the point of a pseudo wall forming. Even lower $AlFA_{50}$ content could possibly result in shorter ignition delays at slower impact speeds, but a full optimization was not pursued.

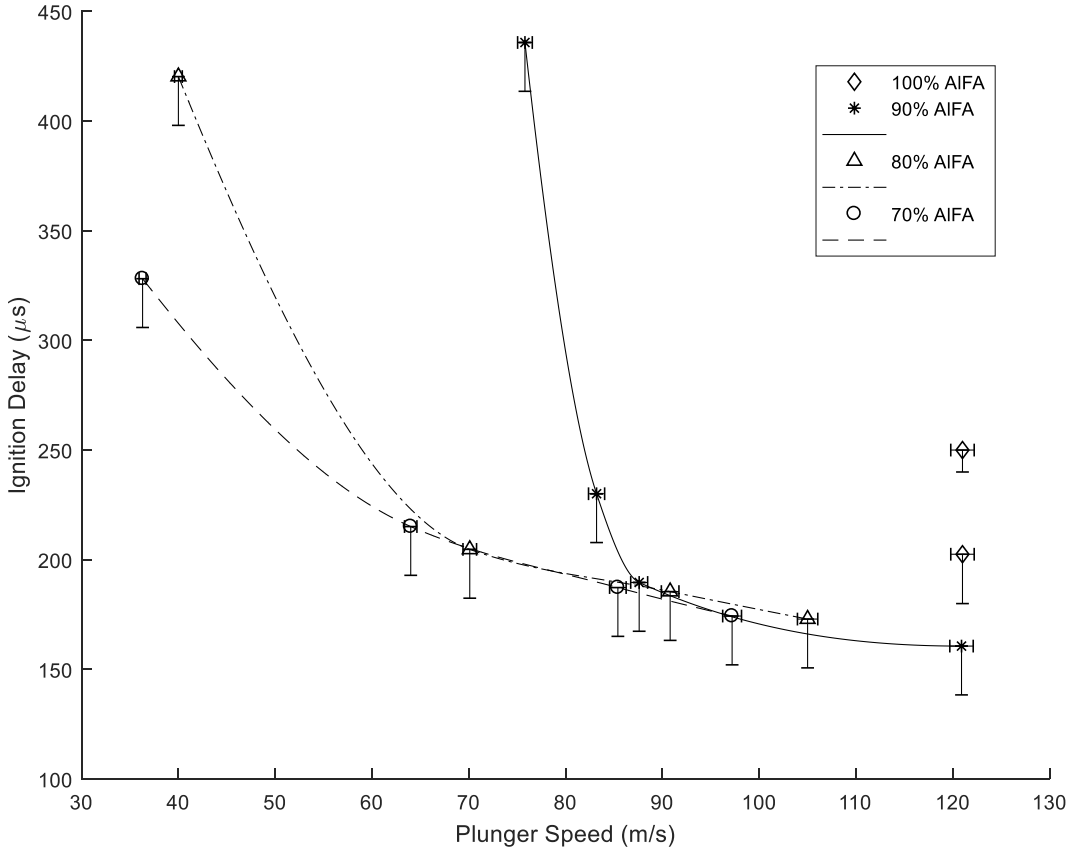

Figure 3.6: Ignition delay from initial impact vs impacting plunger velocity for 70, 80, 90, and 100% $AlFA_{50}$ by volume samples with glass beads. Error on the ignition delay is estimated as 15-20 μs based on the camera frame rate and error on the velocity was determined to be ± 1%.

In short, it was found that this approach was extremely effective and could be tailored to an application to achieve the reliability required and result in a material that has the requisite insensitivities as well. In addition, the direction of the impact would not be expected to be a factor as it might for a mechanical device specifically designed to create a pinch point. Further optimization could be pursued for specific applications but that was beyond the scope of this work.

CHAPTER 4. CONCLUSION

Neat $AlFA_{50}$ has been shown to go through three distinct phases during an impact event in the shear setup of these tests: impact, penetration and extrusion, then ignition. The secondary phase has been shown to be the leading cause of unsuccessful ignition as the impacting plunger is slowed through the melted material, preventing an adequate pinch point from occurring. The importance of a pinch point in a non-shock initiation of this reactive material was demonstrated in modified back plate tests, consistent with the interpretation by White et al. [22]. The introduction of micro-balloons, a classical means for sensitizing liquid explosives, yielded no measurable increase in the sensitivity to impact as sufficiently fast void collapse was not experience at these low impact velocities. Recovered tests of failed micro-balloon additive samples provided more evidence of melting of the sample during the secondary phase. Inclusion of glass beads into the samples was shown to successfully sensitize the $AlFA_{50}$ sample to impact velocities as low as 35 m/s. Two possible mechanisms by which the glass bead additives cause sufficient pinch point were inferred to be interparticle pinching or pinching between a pseudo wall of glass beads and the plunger face. Lastly, it has been shown that by varying the volume of glass bead filler added to the samples, the sensitivity of the sample to impact changes dramatically, and importantly indicates a tailored response is possible at lower impact speeds. This final observation opens the possibility for the material to be sensitized for various applications, or have regions of increased sensitivity which are localized [26].

REFERENCES

[1] R.K. Eckhoff, *Explosion Hazards in the Process Industries*, Gulf Professional Publishing **2016**, p. 385-414.

[2] J.E. Field, G.M. Swallowe, S.N. Heavens, Ignition Mechanisms of Explosives During Mechanical Deformation, *Proc. R. Soc. Lond.* **1982,** 382, 231-244.

[3] S.Y. Ho, Impact Ignition Mechanisms of Rocket Propellants, *Combust. Flame* **1992**, 91, 131–142.

[4] J.E. Field, Hot Spot Ignition Mechanisms for Explosives, *Acc. Chem. Res.* **1992,** 25, 489–496.

[5] C.S. Coffey, V.F. DeVost, D.L. Woody, Towards Developing the Capability to Predict the Hazard Response of Energetic materials Subjected to Impact in:, *Ninth Symp. Detonation*, **1989**, pp. 1243–1252.

[6] V.F. DeVost, C.S. Coffey, Impact Testing of Explosives and Propellants, *Propellants, Explos. Pyrotech*. **1995,** 20, 105–115.

[7] C.S. Coffey, Initiation of Explosive Crystals by Shock o impact in:, *Ninth Symp. Detonation*, **1989**, 58-65.

[8] C.M. Tarver, S.K. Chidester, A.L. Nichols, Critical Conditions for Impact- and Shocked-Induced Hot Spots in Solid Explosives, *J. Phys. Chem.* **1996,** 100, 5794–5799.

[9] A.M. Mellor, D.A. Weigand, K.B. ISOM, Hot Spot Histories in Energetic Materials, *Combust. Flame* **1995**, 101, 26–35

[10] R.B. Frey, *The Initiation of Explosive Charges by Rapid Shear*, Report AD-A090391,Ballistics Research Laboratory Aberdeen Proving Ground, MD, USA **1980**.

[11] M.-A. Fardin, T.J. Ober, C. Gay, G. Grégoire, G.H. McKinley, S. Lerouge, Potential "Ways of Thinking" About the Shear-Banding Phenomenon, *Soft Matter* **2012**, 8, 910–922.

[12] G.T. Afanas, V.K. Bobolev, *Initiation of Solid Explosives by Impact*, Report NASA TT F-623, **1971**.

[13] N.K. Bourne, J.E. Field, Explosive Ignition by the collapse of Cavities, *Proc. R. Soc. A Math. Phys. Eng. Sci.* **1999,** 455, 2411–2426.

[14] R.B. Frey, *Cavity Collapse in Energetic Materials*, Report AD-A172513,Ballistic Research Laboratory Aberdeen Proving Ground, MD, USA **1986**.

[15] C. Wayne, Nitromethane Explosive With A Foam and Microspheres of Air, Patent US3794534A, **1972**.

[16] M. Cartwright, D. Lloyd-Roach, P.J. Simpson, Non-Solid Explosives for Shaped Charges 1: Explosive Parameters Measurements for Sensitized liquid Explosives, *J. Energ. Mater.* **2007**, 25, 111–127.

[17] C.A. Crouse, Fluorinated Polymers as Oxidizers for Energetic Composites, *ACS Symp. Ser.*, **2012**, 1106, 127–140

[18] S. Nandagopal, M. Mehilal, M.A. Tapaswi, S.N. Jawalkar, K.K. Radhakrishnan, B. Bhattacharya, Effect of Coating of Ammonium Perchlorate with Fluorocarbon on Ballistic and Sensitivity Properties of AP/A1/HTPB Propellant, *Propellants, Explos. Pyrotech.* **2009**, 34, 526–531

[19] R.J. Jouet, A.D. Warren, D.M. Rosenberg, V.J. Bellitto, K. Park, M.R. Zachariah, Surface Passivation of Bare Aluminum Nanoparticles Using Perfluoralkyl Carboxylic Acids, *Chem. Mater.* **2005**, 17, 2987–2996

[20] E.M. Hunt, S. Malcom, M.L. Pantoya, F. Davis, Impact Ignition of Nano and Micron Composite Energetic Materials, *Int. J. Impact Eng.* **2009**, 36, 842–846

[21] C.A. Crouse, C.J. Pierce, J.E. Spowart, Synthesis and Reactivity of Aluminized Fluorinated Acrylic (AlFA) Nanocomposites, *Combust. Flame* **2012**, 159, 3199-3207 .

[22] B.W. White, C.A. Crouse, J.E. Spowart, B. Aydelotte, N.N. Thadhani, Impact Initiation of Reactive Aluminized Fluorinated Acrylic Nanocomposites,*J. Dyn. Behav. Mater.* **2016**, 2, 259–271.

[23] R.V. Reeves, A.S. Mukasyan, S.F. Son, Thermal and impact Reaction Initiation in Ni/Al Heterogeneous Reactive Systems, *J. Phys. Chem. C* **2010**, 114, 14772–14780.

[24] R.V. Reeves, A.S. Mukasyan, S.F. Son, Transition from Impact-induced Thermal Runaway to Prompt Mechaonchemical Explosion in Nanoscaled Ni/Al Reacive Systems, *Propellants, Explos. Pyrotech.* **2013,** 38, 611–621.

[25] R.V. Reeves, *Control of Ignition and Reaction Behavior in Gasless Reactive Systems Via Microstructural Modification*, Doctoral Thesis, Purdue University, West Lafayette IN, **2011**.

[26] I.A.J. Shelburne, I.E. Gunduz, S.F. Son, L.A. Morris, C.D. Haines, Sensitization of an Aluminized Fluorinated Acrylic (AlFA) Nanocomposite to an Impact, *Paper in Review for Publication*